INFLUENCE OF MAXIMUM PORE SIZE ON THE FATIGUE PERFORMANCE OF PM STEEL

Anders Bergmark
Höganäs AB, Sweden

Abstract
Two material models for prediction of the fatigue performance of PM steels are compared. The Murakami model considers Vickers hardness and maximum defect (pore) size. The fracture mechanics model includes defect (crack) size and threshold stress intensity factor. Both models shall be considered simultaneously and the combination gives a good prediction of PM steel fatigue limit.
Keywords: PM-steel, fatigue performance, fracture mechanics, Murakami model, defect area

Introduction

The fatigue performance of PM steel has traditionally been considered to be mainly a function of the porosity (density). Increased density has often been seen to be the ultimate way to reach high mechanical performance. However, this one-eyed view shadows the possibilities that can be achieved by a much more detailed insight in the mechanical behaviour of PM. The ongoing competition to conquer and exchange components traditionally manufactured in wrought steel with PM do not necessary mean that increased density is the only way. A more modulated view on the different factors that influence the fatigue performance of PM steel can give guidelines for increased performance that allows the material to be used for high loaded applications already at densities around 7.1 g/cm^3.

Future expansion of PM is also a question of acceptance and available performance data that directly can be used in the design process. A huge amount of data on PM steel fatigue performance is available already. More information and deeper understanding of the mechanisms involved is, however needed. Both theoretical and experimental work is necessary in this process. The scope of this paper is to compare two different models that describe the relation between fatigue performance and internal defects in the material and to compare the model predictions with results from fatigue tests on PM steel. The two models are classic linear elastic fracture mechanics (LEFM) and the Murakami model [1]. The models have originally been developed for solid (continuum) materials containing flaw like defects. Results from fracture mechanics tests on PM steel are available and this allows the fracture mechanics model to be used directly. The Murakami model that predicts the fatigue limit from material macro-hardness, projected (in the direction of the maximum tensile stress) defect area and defects site (surface or internal) has here been modified and includes Young's Modulus as the fourth parameter. The defect area of PM steel is in both models considered to be the projected area of the convex envelope of a large pore or pore agglomerate.

First of all, the models are intended to be used for pre-alloyed PM steels with homogeneous distribution of the alloying elements. The models are not expected to work well on pre-mixed or diffusion-alloyed PM steels with a heterogeneous distribution of the alloying elements along the sinter-necks. Fractography on heterogeneous PM steels often show that fatigue cracks are not originating from pores [2,3,4].

Both models have initiation defect size and site as parameters. Fractography of one AstaloyCrL sample to find these parameters is discussed in detail after the presentation of the two models.

Fracture Mechanics Model

Fracture mechanics considers the stress intensity factor as the controlling parameter. Cyclic loading of pre-cracked test bars is used to find the relation between variation of the stress intensity factor ΔK_I and crack growth characteristics. Of special interest here is the lower limit of $\Delta K_I = \Delta K_{Ith}$ that gives a crack growth rate of the order $da/dN < 10^{-8}$ m/cycle, i.e. <10 nm per load cycle. Several investigation on quantified threshold values are presented in the literature. Typically, the threshold value is 8 – 10 MPa√m for PM steel. The threshold-value is relatively independent on both type of PM steel and density in the interval 7.1 g/cm^3 to full density [5,6].

Consider pores as cracks where the crack size corresponds to the projected area of the pore. Assume a quarter-circle corner crack, a half-circle edge crack and a full circle internal crack. Also assume that the cracks are small compared to the dimensions of the cross-section.

The stress intensity factor of axially loaded and/or bended bars with cracks close to the surface is:

$$K_I = f \cdot \sigma_\infty \sqrt{\pi a} \tag{1}$$

where σ_∞ is remote stress and a is radius of the corner-, edge- or internal crack. f is a factor depending on the type of crack. Corner cracks (quarter circle) have $f \approx 0.72$ [7], edge (half-circle)- and embedded (circle) cracks have $f \approx 0.65$ [8].

The projected crack surfaces are:

$$Area_{corner} = \frac{1}{4}\pi a_c^{\,2}; \qquad Area_{edge} = \frac{1}{2}\pi a_e^{\,2}; \qquad Area_{\text{int}} = \pi a_i^{\,2};$$

Assume that all cracks have the same projected area.

$$\Rightarrow a_c = \sqrt{2} \cdot a_e = 2 \cdot a_i$$

The same ΔK_{Ith} for all three positions of the crack-like pore implies different remote (combination of axial and bending) stresses:

$$0.72 \cdot \sigma_{c\infty} \sqrt{\pi a_c} = 0.65 \cdot \sigma_{e\infty} \sqrt{\pi a_e} \qquad \Rightarrow \sigma_{e\infty} \approx 1.32 \cdot \sigma_{c\infty} \tag{2}$$

The relation between edge and internal cracks is obtained in the same way:

$$\sigma_{i\infty} \approx 1.19 \cdot \sigma_{e\infty}, \; \sigma_{i\infty} \approx 1.57 \cdot \sigma_{c\infty} \qquad (3)$$

I.e. the remote stress is increased by 32% when corner cracks are eliminated and about 57% when both corner and edge cracks are eliminated for constant stress intensity factor. It is obvious that corner defects must be avoided in order to obtain high performance of PM components. Test on circular test bars gives 19% increased performance when the detrimental effect from surface defects are neutralized.

The cyclic stress amplitude that is the upper bound for the fatigue endurance limit at the same load ratio is calculated from (1) where the cyclic stress amplitude is $\sigma_F = \Delta\sigma_\infty /2$.

Murakami Model

The Murakami model is developed for homogeneous solid materials and includes three parameters: Vickers (macro) hardness, defect area and a factor that considers the site of the initiation defect. The defect area is defined as the convex envelope of the physical discontinuity that initiates the onset of crack growth. Typical defects might be an inclusion, cavity, soft grain in a hard matrix, grain boundary precipitation etc. The predicted fatigue limit is:

$$\sigma_M = const \cdot \frac{H_V + 120}{\sqrt[12]{area}} \qquad (4)$$

where *const* = 1.41 for edge defects and *const* = 1.56 for internal defects. The Murakami model is empirical and predicts about 10% increased performance when edge defects are eliminated. The predicted fatigue limit is valid for rotating bending, i.e. load ratio R=-1.

PM steel Hardness in the Murakami Model

The macro-hardness of PM steel is a combination of hardness of the metallographic phases and the porosity. Increased porosity gives lower macro-hardness for the same microstructure. A separation of the influence of microstructure and porosity (density) is of great value both for the development of PM steels and for the design process for components where these factors can be chosen more or less independently.

Hardness for PM steel is often available as micro hardness HV0.1 or HV0.05 of the different phases contained in the matrix. The micro-hardness is a characteristic of separate metallographic phases and is not influenced by the porosity. A modification of the Murakami model will be introduced by considering the influence of the pores via the Young's Modulus.

Modified Murakami Model for PM steel

Consider the defect area to be contained in a small volume here called the initiation volume. All micro-mechanisms involve in the initial crack growth are assumed to take place in the initiation volume [9]. The projected defect area in PM steel typically corresponds to diameter 0.2 mm circle and the initiation volume is slightly larger than the defect itself. A typical cross-section of a fatigue test bar exceeds 5 x 5 mm^2. I.e. the projected area of the initiation volume is much smaller than the cross-section.

Onset of crack growth takes place when the initiation volume is subjected to a critical macroscopic strain. The load carried by the initiation volume is much smaller than the load carried by the entire cross-section. Information about presence of pores in the bulk of the material can only be transferred to the initiation volume via the Young's Modulus. Decreased Young's Modulus will increase the strain and the fatigue limit will be reduced in direct relation to the change of the Young's Modulus. A modification of the Murakami model is introduced in (5) below:

$$\sigma_{M,\text{mod}} = const \cdot \frac{H_{V,micro} + 120}{\sqrt[12]{area}} \cdot \frac{E_p}{E_0} \tag{5}$$

where E_p and E_0 are the Young' Modules of the porous and full dense materials respectively. There are several empirically based models for the relation between PM steel density and Young's Modulus. The MacAdam model [10] gives the relation directly between the density and Young's Modulus:

$$E_p = E_0 \left(\frac{\rho_p}{\rho_0} \right)^m \tag{6}$$

The numerical parameter *m* is empirically found to be close to 3.4 [9,10]

Fatigue crack initiation in PM steel

Both models presented contain the projected defect area and the position of the initiation as parameters. What is the size of a typical initiation defect in PM steel and where does is it situated? Fractography of cyclic loaded PM steel show that crack preferably starts in corners [11] when about equally sized large defects are randomly distributed over the cross-section. Initiation at edge pores occurs when an edge pore is considerably larger than corner pores. Initiation from internal pores are very rare in test bars that are tested in the as

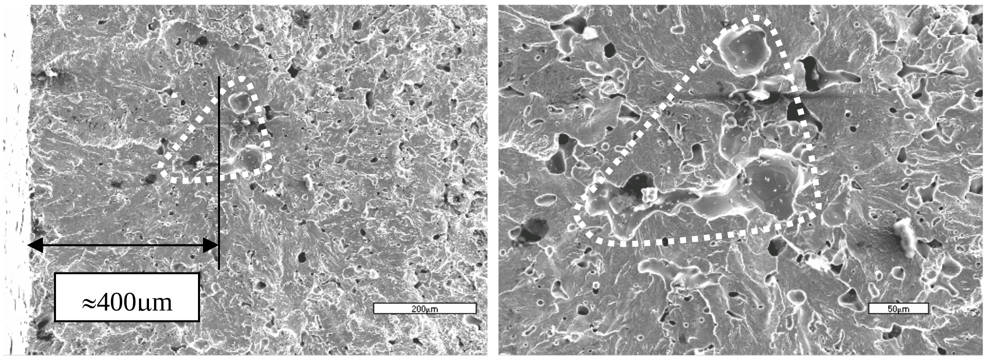

Fig.1. Crack initiation site in shot-peened AstaloyCrL subjected to axial fatigue. The dotted line outlines the convex envelope (marked with dotted line) of the projected initial defect. The defect area is approximately 20.000 μm^2. The bars are 200μm (left) and 50μm (right) respectively.

sintered condition without any modification of the surfaces, by for example machining, shot peening or case hardening. Investigations on microstructures and pore shape are normally performed with light optical microscope on a cross-section. The probability to find the largest defect area in a randomly placed cross-section with the same method is extremely small. The most efficient way to find the initiation site is by fractography. The SEM fractograph presented in Fig. 1 is obtained from a shot-peened test bar in material AstaloyCrL. Shot-peening effectively eliminates crack initiation at the surface of two reasons. Compressive residual stresses are introduced in the surface that reduces the maximum tensile stress and pores open to the surface are closed or considerably reduced in size. Comparative investigations performed at Höganäs AB have shown that internal defects and edge defects are of about the same size in PM steel. The microstructure of the material in the fractograph is characterized by fine pearlite with a micro-hardness of about 500 HV0.1. The material is tested in axial fatigue with load ratio R=-1. The internal initiation site is placed about 400μm below the surface and has the typical characteristics of a fish-eye fracture, i.e. an almost circular light spot surrounded by a grayish area that can be seen directly with the naked eye. These characteristics are optical effects and cannot be seen in the SEM fractographs presented here. The high-resolution fractograph to the right show crack initiation at two internal pores. Crack walk is initially obtained in direction to the left until the crack reaches the specimen surface. The successive crack growth is inter-particle mainly through the sinter-necks and much more pores can be seen outside the initial trans-particle crack walk area. The fatigue test was terminated when the stiffness was reduced by about 15%. The projected defect area is taken as the envelope of the convex area that contains the two pores; see Fig. 1 to the right. The projected defect area is in this case about 20.000 μm^2. This is a typical size of the initiation defect in PM steels at density 7.3 g/cm^3. The plane bending fatigue limit of this material without shot-peening at load ratio R=-1 is 340 MPa.

Combined Models

Diagrams that show the relation between defect area and fatigue performance are presented below for both models. Fig. 2 shows the relation between defect area and predicted fatigue limits for internal defects and Fig. 3 for surface defects.

The modified Murakami model is valid for rotating bending R=-1. Threshold values for ΔK_{Ith} determined by Piotrowski et.al. [4] for load ratios R from R=0.8 to R=-1. A large influence from load ratio was found. ΔK_{Ith} = 10 MPa√m was found for density 7.34 g/cm^3 samples at R=-1 in 0.85% pre-alloyed Mo pre-mixed with 2%Ni and 0.6%C. The difference in ΔK_{Ith} reported in the literature between different alloying systems is small. The diagrams shown below includes the results for ΔK_{Ith} = 6, 8 and 10 MPa√m.

Internal defects

The combined diagram for internal defects is shown in Fig. 2 below.

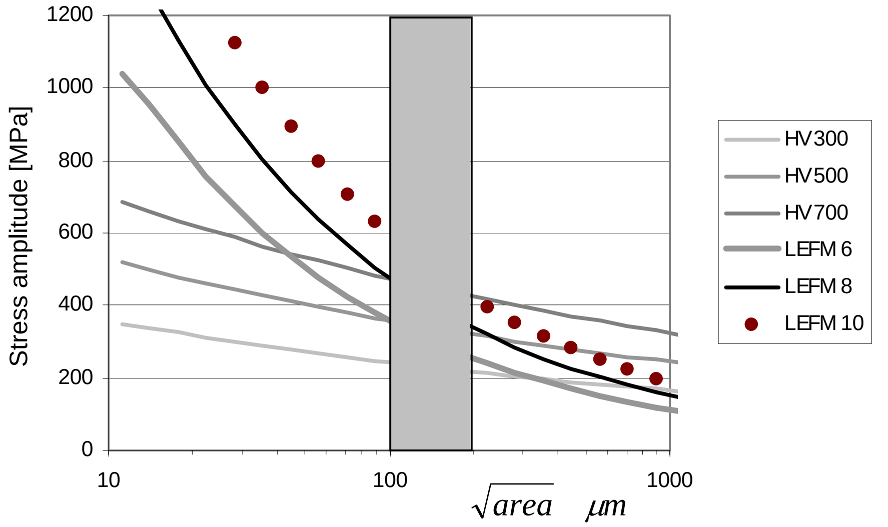

Fig. 2. Combined diagrams for the LEFM and the modified Murakami models valid for internal pores. The shadowed area show typical defect sizes found by fractography in PM steel at densities around 7.3 g/cm^3.

Surface defects
The combined diagram for surface defects is shown in Fig. 3 below.

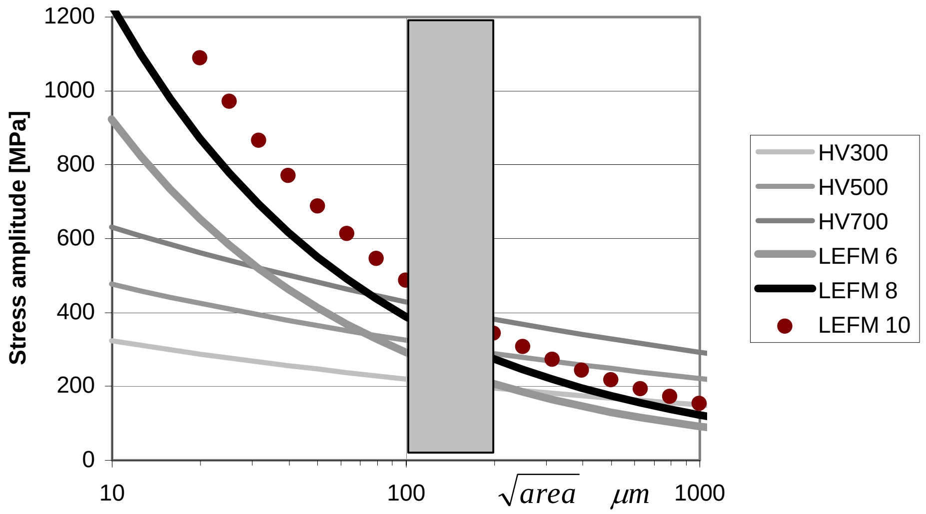

Fig. 3. Combined diagrams for the LEFM and the modified Murakami models valid for surface pores. The shadowed area show typical defect sizes found by fractography in PM steel at densities around 7.3 g/cm^3.

Numerical example
Application of the Murakami model for micro-hardness 500HV0.1 corresponding to the AstaloyCrL material discussed earlier with a 20.000 μm^2 surface pore predicts a fatigue limit of 306MPa. The fatigue performance in plane bending R=-1 is 340MPa, i.e. about 10% higher. The fracture mechanics model with ΔK_{Ith} =8 MPa√m predicts 347 MPa, i.e. slightly higher than the modified Murakami model. See also Fig. 3.

A fully martensitic microstructure increases the micro-hardness above 700 HV0.1. The modified Murakami model prediction then increases to more than 400MPa. The threshold stress intensity factor, however is not influenced by the increased hardness and the material performance is predicted from the fracture mechanics model to 347MPa. The important conclusion that can be drawn from this numerical example is that a relatively low increase in fatigue performance of PM can be expected from through hardened PM steel. This performance level coincides well with what is found in experiments.

Influence of size of defect area

The influence of defect area size is largest for the fracture mechanics model. This is clearly seen in the two diagrams presented above (Fig. 2 and Fig.3). The predicted fatigue limit is inversely proportional to $\sqrt[12]{area}$ in the modified Murakami model and to $\sqrt[4]{area}$ in the fracture mechanics model. The predicted influence of an increased defect area of 50% is 11% for the LEFM model and 3% for the modified Murakami model. The numerical example presented in the section above has shown that increased hardness with the purpose to increase the bending fatigue performance must be combined with measures to get smaller defects. There are also alternate process routes to obtain higher bending fatigue performance by closing surface pores and introduction of compressive residual stresses in the surface. Somewhere, however there is a critical point where the crack initiation will start and smaller initiation defect size will always be beneficial.

Summary

Two models for prediction of fatigue performance of PM steels have been compared. The linear elastic fracture mechanics model (LEFM) is more sensitive to defect size than the Murakami model modified for influence of porosity. Increased hardness raises the predicted fatigue limit in the modified Murakami model. Fatigue tests on AstaloyCrL with microstructure characterized by fine pearlite (500HV0.1) and martensite (>700HV0.1) respectively and defect size about 20.000 μm^2 in both cases, however, only show a minor improvement when micro-hardness is increased. This result is in accordance with the LEFM model for which the limit is set by the defects size. High hardness with the purpose to increase the fatigue performance must, according to the models investigated, be combined with smaller defect size.

References

[1] Y.Murakami, *Metal Fatigue: effects of small defects and nonmetallic inclusions*, Elsevier Science Ltd. Oxford 2002

[2] Anders Bergmark and Luigi Alzati, “Fatigue crack walk in Cu-Ni-Mo alloyed PM steel.” Special issue of Fatigue and Fracture of Engineering Materials and Structures (FFEMS), vol.28, No.1-2, 2005.

[3] A.Bergmark, L.Alzati, U.Persson. “Fatigue crack initiation in PM Steel”, *Advances in Powder metallurgy & Particulate Materials*, compiled by V.Arnhold, CL.Chu, W.F.Jandeska and H.Sanderow. MPIF, Princeton, NJ, 2002, part 5, pp 95-103

[4] L.Alzati, A.Bergmark, J.Andersson, “Micro structural reinforcement obtained by diffusion bonding”, presented at the PM2TEC conference in Montreal June 2005

[5] G.Piotrowski, X.Deng, N.Chawla. “Fatigue Crack Growth of Fe-0.85%Mo-2Ni-0.6C steels with heterogeneous microstructure”. *Advances in Powder Metallurgy & Particulate*

Materials, compiled by B. James and R. Chermenkoff, MPIF Princeton, NJ, 2004, part 10, pp. 86-97
[6] I.Bertilsson, B.Karlsson. “Dynamic properties of sintered steel”, pre-print supplement 1986 Powder Metallurgy group Meeting, Buxton, England, p. 15.1
[7] T.L Anderson. *Fracture Mechanics Fundamentals and Applications*. 2nd edition. CRC Press 1995 p. 627
[8] T.L Anderson. *Fracture Mechanics Fundamentals and Applications*. 2nd edition. CRC Press 1995 p. 631
[9] A.Bergmark, “Influence of Density on PM Steel Fatigue Crack Initiation and Propagation” *Advances of Powder Metallurgy & Particulate Materials – 2001*. Compiled by W.B.Eisen and S.Kassam. MPIF 2001, Part 10, pp. 95-102
[10] MacAdam. “Some relations of powder characteristics to the elastic modulus and shrinkage of sintered ferrous compacts.” *J. Iron Steel Inst*. Volume 168, 1951. pp. 346 – 348.
[11] A.Bergmark and S.Bengtsson “Fatigue Properties of Cu-C alloyed PM Steel at Two Density Levels”. *Euro PM 2001. European Congress and Exhibition on Powder Metallurgy*, Nice France Oct. 22-24. EPMA 2001, Vol. 2, pp.110-115